

A Designed Zinc-finger Transcriptional Repressor of Phospholamban Improves Function of the Failing Heart

H Steve Zhang¹, Dingang Liu², Yan Huang², Stefan Schmidt³, Reed Hickey², Dmitry Guschin¹, Haili Su², Ion S Jovin², Mike Kunis¹, Sarah Hinkley¹, Yuxin Liang¹, Linda Hinh¹, S Kaye Spratt¹, Casey C Case¹, Edward J Rebar¹, Barbara Ehrlich³, Philip D Gregory¹ and Frank J Giordano²

¹Sangamo BioSciences Inc., Richmond, California, USA; ²Department of Cardiovascular Medicine, Yale Medical School, New Haven, Connecticut, USA; ³Department of Pharmacology, Yale Medical School, New Haven, Connecticut, USA

Selective inhibition of disease-related proteins underpins the majority of successful drug–target interactions. However, development of effective antagonists is often hampered by targets that are not druggable using conventional approaches. Here, we apply engineered zinc-finger protein transcription factors (ZFP TFs) to the endogenous phospholamban (*PLN*) gene, which encodes a well validated but recalcitrant drug target in heart failure. We show that potent repression of *PLN* expression can be achieved with specificity that approaches single-gene regulation. Moreover, ZFP-driven repression of *PLN* increases calcium reuptake kinetics and improves contractile function of cardiac muscle both *in vitro* and in an animal model of heart failure. These results support the development of the *PLN* repressor as therapy for heart failure, and provide evidence that delivery of engineered ZFP TFs to native organs can drive therapeutically relevant levels of gene repression *in vivo*. Given the adaptability of designed ZFPs for binding diverse DNA sequences and the ubiquity of potential targets (promoter proximal DNA), our findings suggest that engineered ZFP repressors represent a powerful tool for the therapeutic inhibition of disease-related genes, therefore, offering the potential for therapeutic intervention in heart failure and other poorly treated human diseases.

Received 1 May 2011; accepted 2 April 2012; advance online publication 24 July 2012. doi:10.1038/mt.2012.80

INTRODUCTION

Effective human therapies typically require an agent that blocks function of a pathological gene product. Development of such agents can be problematic if the drug target—which is typically a protein—is located in an inaccessible cellular compartment, or presents a mechanism of action that is not readily disrupted. Addressing the gap between known and druggable disease targets requires a methodology that can circumvent such limitations; this consideration has kindled great interest in methods

capable of decreasing the cellular levels of these targeted proteins by suppressing their expression (e.g., the use of RNA interference technology to suppress the translation of targeted mRNAs). It has been demonstrated that human genes implicated in disease may be regulated by targeting genomic DNA using designed zinc-finger transcription factors (ZFP TFs) composed of an engineered zinc-finger DNA-binding domain specific for the gene of interest fused to a relevant functional domain (reviewed in ref. 1). We and others have previously shown that designed ZFP TFs can evoke therapeutic activation of gene expression *in vivo*.^{2–5} ZFP repressors have also been reported to function in a tumor xenograft model and in mouse retina against a human transgene.^{6,7} However, as a class of therapeutic molecules that have the potential to provide antagonist activity to the large body of nondruggable targets, ZFP repressors have not been tested extensively *in vivo*, especially in the context of *bona fide* endogenous genes and delivery to native organs/tissues.

Phospholamban (*PLN*), a 52 amino acid protein, plays a critical role in the kinetics of calcium flux in cardiac muscle. It inhibits the activity of the sarcoplasmic reticulum calcium ATPase (*SERCA2a*),⁸ which returns cytosolic calcium into sarcoplasmic reticulum after each contractile cycle in preparation for subsequent excitation-contraction events.⁹ Decreased *SERCA2a* activity, either as a result of reduced expression, increased *PLN* expression, or *PLN* mutations that superinhibit *SERCA2a* function has been associated with human heart failure.^{10–13} Conversely, increasing the *SERCA2/PLN* ratio in cardiomyocytes, either by reducing *PLN* levels or increasing *SERCA2* levels, markedly improves both the systolic contraction and diastolic relaxation of cardiac muscle.^{14–18} Moreover, dominant-negative *PLN* strategies that interfere with the *PLN*–*SERCA2* interaction have proven effective in augmenting *SERCA2* function and cardiac contractility in animal models.¹⁹ Importantly, unlike β -agonists, direct targeting of *SERCA2* or *PLN* enhances contractility without concomitant activation of the entire β -adrenergic pathway, which has been shown to increase mortality in congestive heart failure patients. While inhibition of *PLN* provides an attractive approach for improving cardiac function, its mechanism of action (as an inhibitor of *SERCA2a*)

D.L. and Y.H. contributed equally to this work.

Correspondence: Frank J Giordano, Department of Cardiovascular Medicine, Yale University, Rm. 437, 10 Amistad, New Haven, Connecticut 06520, USA. E-mail: frank.giordano@yale.edu

and location within an organelle membrane combine to make it a difficult target for standard small molecule or antibody-based methods.²⁰ We sought to determine whether engineered ZFP TFs can be applied to the *PLN* gene to achieve therapeutically relevant gene repression and enhancement of cardiac function.

RESULTS

Design and *in vitro* testing of ZFP TFs

Rat H9C2(2-1) cells are derived from heart tissues and express detectable levels of *PLN*, therefore were chosen as a cell culture model for identifying ZFP repressors of *PLN*. ZFP designs were focused on a region of accessible chromatin as revealed by mapping of *DNaseI* hypersensitive sequences. In H9C2(2-1) cells, a single accessible region was identified between bases -2,350 and -2,050 relative to the transcription start site (Figure 1a).

This region included a span of enhanced sequence conservation between rat and human, suggesting regulatory significance. ZFP TFs were engineered to bind five distinct 18-bp targets within this region. Each ZFP comprised six fingers, and was constructed from an archive of 2-finger units as previously described.²¹ Such ZFPs have demonstrated a capacity for potent target repression *in vitro* with single-gene specificity in expression profiling studies.²² Each was then linked to the Krüppel-associated box (KRAB A/B) repression domain from the N-terminal region of the KOX1 protein to create a ZFP TF repressor (Figure 1b). Transient transfection of plasmid DNAs encoding these ZFP TFs into H9C2(2-1) cells demonstrated up to an 80% reduction in *PLN* mRNA, with the protein 6439-KOX reproducibly exhibiting the greatest degree of repression (Figure 1c). Further studies of this protein indicated that its repressive effect was dependent upon the functional

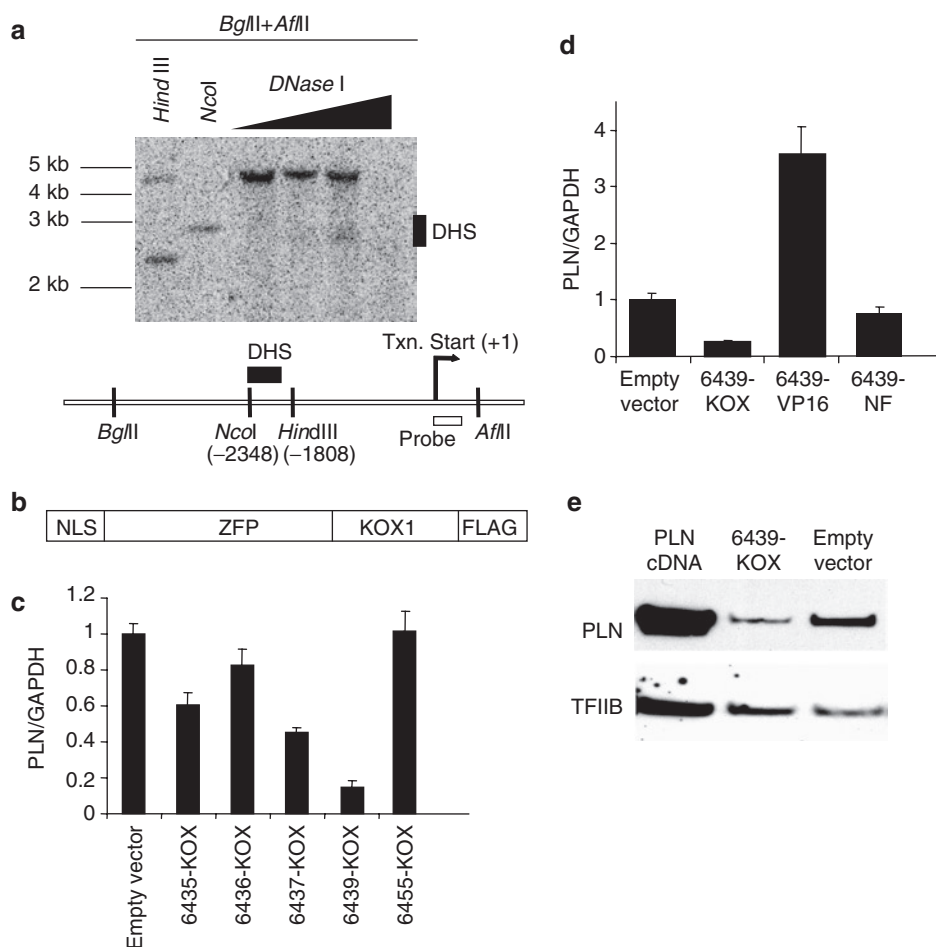


Figure 1 Targeting and *in vitro* analysis of zinc-finger protein transcription factor (ZFP TF) repressors of the rat phospholamban (*PLN*) gene. **(a)** Nuclei of H9C2(2-1) cells were isolated and titrated with *DNaseI* (Worthington) as described.³ Isolated genomic DNA was double-digested with *Bgl*II and *Afl*II. Aliquots of double-digested DNA were subjected to *Hind*III or *Nco*I digest for use as genomic size markers. The location of the *DNaseI* hypersensitive region (DHS) is indicated by a solid bar next to the blot and in the schematic diagram. The transcription start site (+1) is marked by the hooked arrow. The nucleotide locations of the *Nco*I site and the *Hind*III site are relative to the transcription start site. The open box indicates the location of the probe for Southern blot. **(b)** The structure of the assembled ZFP repressors is depicted in the diagram. NLS, nuclear localization signal; KOX1, repression domain of KOX1; FLAG, FLAG epitope tag. **(c)** H9C2(2-1) cells were transiently transfected with plasmids expressing the indicated ZFP TFs (**Supplementary Materials and Methods**). After 72 hours mRNA was harvested and the levels of *PLN* mRNA and *GAPDH* mRNA were quantified using real-time reverse transcription (RT)-PCR (Taqman). The *PLN* level was normalized to that of *GAPDH*. **(d)** Variants of the 6439-KOX repressor protein in which the KOX repression domain was either removed (6439-NF) or replaced with an activator (6439-VP16), were tested for function in H9C2(2-1) cells. *PLN* mRNA levels were measured as in **(b)**. **(e)** H9C2(2-1) cells were transiently transfected as indicated, and 72 hours later whole cell extracts were collected and subjected to western blot analysis. A *PLN* cDNA was used as a positive control for the anti-*PLN* antibody.

domain since removal of the KOX moiety eliminated repression and replacement with the VP16 activation domain increased PLN mRNA levels (Figure 1d). Western blot analysis confirmed that 6439-KOX also reduced PLN protein levels (Figure 1e). Together, these results demonstrate that 6439-KOX is a potent and domain-dependent repressor of *PLN*.

ZFP-driven *PLN* repression is highly specific

6439-KOX recognizes an 18-bp sequence that is unique within the rat genome, theoretically permitting function with singular specificity. We conducted DNA microarray experiments to determine the genome-wide impact of 6439-KOX on gene expression. The genes regulated by 6439-KOX (as determined by the software) in two independent transfections are listed in Table 1a and b. No gene was found to be activated. Only two genes, *PLN* and *ankyrin repeat domain 24* (predicted), were found to be repressed in both experiments. The regulation of *PLN* (2.05-fold and 1.99-fold) is more pronounced than that of the other gene (1.71 fold and 1.74 fold). The smaller fold of repression for *PLN* as measured by microarray (relative to the approximately fivefold-repression measured by real-time reverse transcription-PCR (Supplementary Figure S1) likely reflects differences in how RNA levels are measured in these two distinct assays. Specifically, the fold of repression may be underestimated in the microarray experiment because the *PLN* levels (120–155 fluorescence units in control samples and 61–78 units in ZFP-treated samples, as measured by the scanner) is near the lower end of the signal range genome-wide (10–25,000 fluorescence units). The repression of catecholamine-O-methyltransferase observed in the first microarray experiments could not be confirmed by Taqman analysis (Supplementary Figure S1), therefore is likely a result of aberrant detection of the microarray. These data demonstrate that the engineered TF 6439-KOX functions with high specificity within the monitored genome, with *PLN* potentially being the only gene that is significantly regulated.

Designed *PLN* repressor accelerates calcium transients and improves contractility

As a more rigorous and therapeutically relevant test of function, we examined the activity of 6439-KOX in primary rat cardiomyocytes. Cardiomyocytes are the target cell type for treating heart failure and express much higher levels of *PLN* than H9C2(2-1) cells. Accordingly, primary cardiomyocytes isolated from day 1 neonatal rats were transduced with recombinant adenovirus encoding either 6439-KOX (Ad-6439-KOX) or the KOX repression domain alone (Ad-KOX). Under conditions yielding >85% transduction, Ad-6439-KOX repressed *PLN* mRNA levels by up to 75% relative to Ad-KOX (Figure 2a). Western blot analysis confirmed a significant reduction in *PLN* protein levels by 6439-KOX (Figure 2b), demonstrating potent inhibition of the *PLN* promoter even in its highly induced native state in cardiomyocytes.

To determine whether this level of *PLN* repression would be sufficient to elicit the anticipated effects on calcium handling, neonatal rat cardiomyocytes were transduced with either Ad-6439-KOX or Ad-KOX, and 48 hours later calcium transients were measured in electrically paced cardiomyocytes loaded with the calcium fluorophore Fluo-3. The times needed to reduce the cytosolic calcium levels to 50% of the peak levels ($T_{1/2}$) (Figure 2c) and to 5% of the peak levels (Figure 2d) were significantly decreased in Ad-6439-KOX-treated cells relative to control cells, indicating an increased rate of calcium removal from the cytosol during each pacing cycle that is consistent with reduced *PLN* levels and enhanced SERCA2a activity.

To analyze the effects of 6439-KOX on contractility at the single-cell level we carried out an *in vivo* direct intramyocardial coinjection of either Ad-6439-KOX and Ad-FS-Red (an adenovirus encoding a fluorescent marker, FS-Red) or Ad-KOX and Ad-FS-Red. We and others have previously observed that when delivering two distinct adenoviral vectors simultaneously a high-cotransduction rate occurs (Supplementary Figure S2).²³

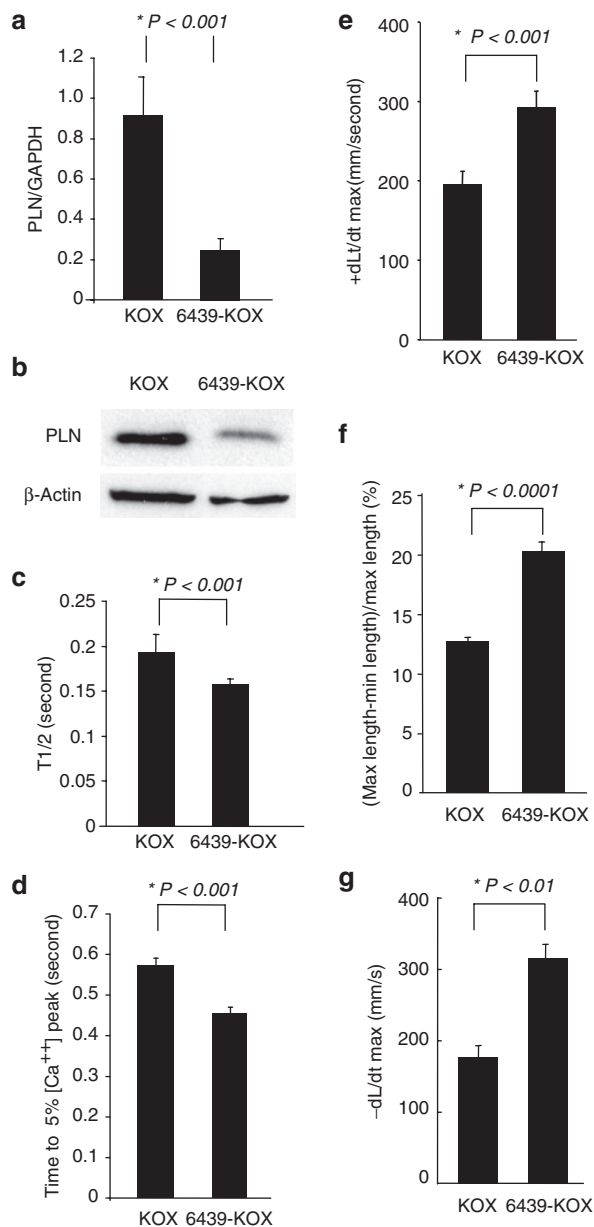
Table 1 Specificity of the ZFP repressor of *PLN*

a						
Probe	RNA levels		Fold repression	Statistics		
	Empty vector	6439-KOX		Confidence down %	T-Test	P value
1368826_at	917.75	238.05	3.86	100	0.04	Catecholamine-O-methyltransferase
1370157_at	124.7	60.9	2.05	100	0.013	Phospholamban
1372499_at	486.15	284.3	1.71	100	0.038	Ankyrin repeat domain 24 (predicted)
1369215_a_at	1,191.40	779.9	1.53	100	0.05	Carboxypeptidase D precursor
b						
Probe	RNA levels		Fold repression	Statistics		
	Empty vector	6439-KOX		Confidence down %	T-test	P value
1370157_at	154.85	77.9	1.99	100	0.006	Phospholamban
1372499_at	662.1	380.25	1.74	100	0.004	ankyrin repeat domain 24 (predicted)
1374446_at	1,800.95	1,615.15	1.12	100	0.03	TCDD-inducible poly(ADP-ribose) polymerase (predicted)

Microarray analysis were performed for two independent transfections (a and b). For each transfection, a plasmid-encoding 6439-KOX or the empty vector was transfected into H9C2(2-1) cells in duplicate, and RNA isolated 60 hours post-transfection. The genes that are called as “changed” by the software (100% confidence, which means all four comparisons between duplicate ZFP and control samples show regulation of the gene and $P < 0.05$) for the two experiments are listed. No genes were found to be activated.

PLN, phospholamban; ZFP, zinc-finger protein.

Thus, FS-Red labeled cells are likely to be also successfully transduced with the test adenoviral vectors. At 72 hours postinjection, hearts were explanted and cardiomyocytes isolated, and the contractility of individual FS-Red-positive cardiomyocytes was determined by an edge detection method during electrical pacing.²⁴ As shown in **Figure 2e**, cardiomyocytes transduced with Ad-6439-KOX exhibited a highly significant enhancement in the maximum rate of lengthening when compared to cells isolated following injection of the Ad-KOX vector, consistent with the expected increase in SERCA2a activity in these cells. Moreover, both the extent of cell shortening (**Figure 2f**) as well as the rates of shortening (**Figure 2g**) were also significantly improved in cells transduced with Ad-6439-KOX. These data demonstrate that at the individual cardiomyocyte level, ZFP-mediated *PLN* repression is sufficient to drive a phenotype of enhanced calcium transient and contractility.



ZFP-driven *PLN* repression improves heart function, alters the hypertrophic response, and reduces post-infarction cardiac dysfunction

To test the *in vivo* efficacy of the *PLN* repressor we used a rat model of sequential cardiac pressure overload and myocardial infarction, allowing us to assess the effects of *PLN* repression on two commonly encountered clinical pathophysiological states. Pressure overload was induced by ligation-induced stenosis of the abdominal aorta between the renal arteries. The degree of stenosis was standardized surgically and corroborated by Doppler flow analysis across the stenotic region. We used this model as it induces not only pressure overload, but also alterations in the renin-angiotensin system that have been associated with heart failure.²⁵ Before aortic constriction we performed gene delivery to the heart by direct multistep intramyocardial injection of adeno-associated virus serotype 2 vectors (AAV-2) expressing either 6439-KOX or β -galactosidase (as control). Intramyocardial injection of AAV- β -gal in this manner resulted in expression primarily restricted to portions of the anterior and lateral walls of the left ventricle (**Supplementary Figure S3**). Evaluation by echocardiography 4.5 weeks later revealed that the rats injected with AAV-6439-KOX had augmented cardiac contractile function (as measured by fractional shortening; **Figure 3a**), and an attenuated hypertrophic response (less thickening of the ventricle wall, **Figure 3b**). These observations are consistent with the predicted phenotype of *PLN* repression and increased SERCA2a activity which include reduced hypertrophy.^{9,26} Interestingly, whereas end-diastolic diameters were unchanged from baseline in the 6439-KOX-treated hearts at 4.5 weeks post-aortic banding, they were reduced significantly in the AAV- β -gal hearts that received aortic banding (**Figure 3c**), possibly secondary to a greater hypertrophic response in these hearts.

As a further test of 6439-KOX's ability to preserve cardiac function after a pathophysiological insult, we induced myocardial infarction in these same rats 4.5 weeks after aortic constriction. Infarction was induced by ligation of the left anterior descending coronary artery, the major blood supply of the anterior wall of the left ventricle. Fourteen-days later, terminal hemodynamic

Figure 2 Zinc-finger protein (ZFP)-driven repression of phospholamban (*PLN*) improves calcium transient and contractility in rat cardiomyocytes. (**a,b**) Cultured neonatal rat cardiomyocytes were transduced with adenoviral vectors encoding either the *PLN* repressor ZFP (6439-KOX) or the repressor domain alone without the ZFP DNA-binding domain (KOX) at MOI 200. Seventy-two hours later, *PLN* (**a**) mRNA levels and (**b**) protein levels were measured. (**c,d**) Cultured neonatal rat cardiomyocytes infected with either Ad-6439-KOX or Ad-KOX were loaded with Fluo-3 and calcium transients were assessed during excitation-contraction induced by electrical pacing. The rate of calcium reuptake into the sarcoplasmic reticulum was measured as the time required to decrease cytosolic calcium levels to (**c**) 50% or (**d**) 5% of their peak after depolarization. ($n = 25$ for KOX-transduced cells, $n = 25$ for 6439-KOX-transduced cells). (**e,f**) Either Ad-6439-KOX or Ad-KOX, mixed with an equal titer of Ad-FS-Red (an adenoviral vector encoding a Fluorescent marker) were codelivered to rat hearts via direct intramyocardial injections. Cardiomyocytes were isolated 72 hours after injection, and edge-detection-based analysis of single-cell contractility during electrical stimulation was performed on FS-Red-positive cells. The rate of (**e**) cell lengthening (relaxation), (**f**) percent cell shortening and the (**g**) rate of cell shortening (contraction) were determined ($n = 15$ cells per group three separate injected hearts per treatment; five cotransduced cells per heart examined; and at least five separate contraction-relaxation cycles were analyzed per cell).

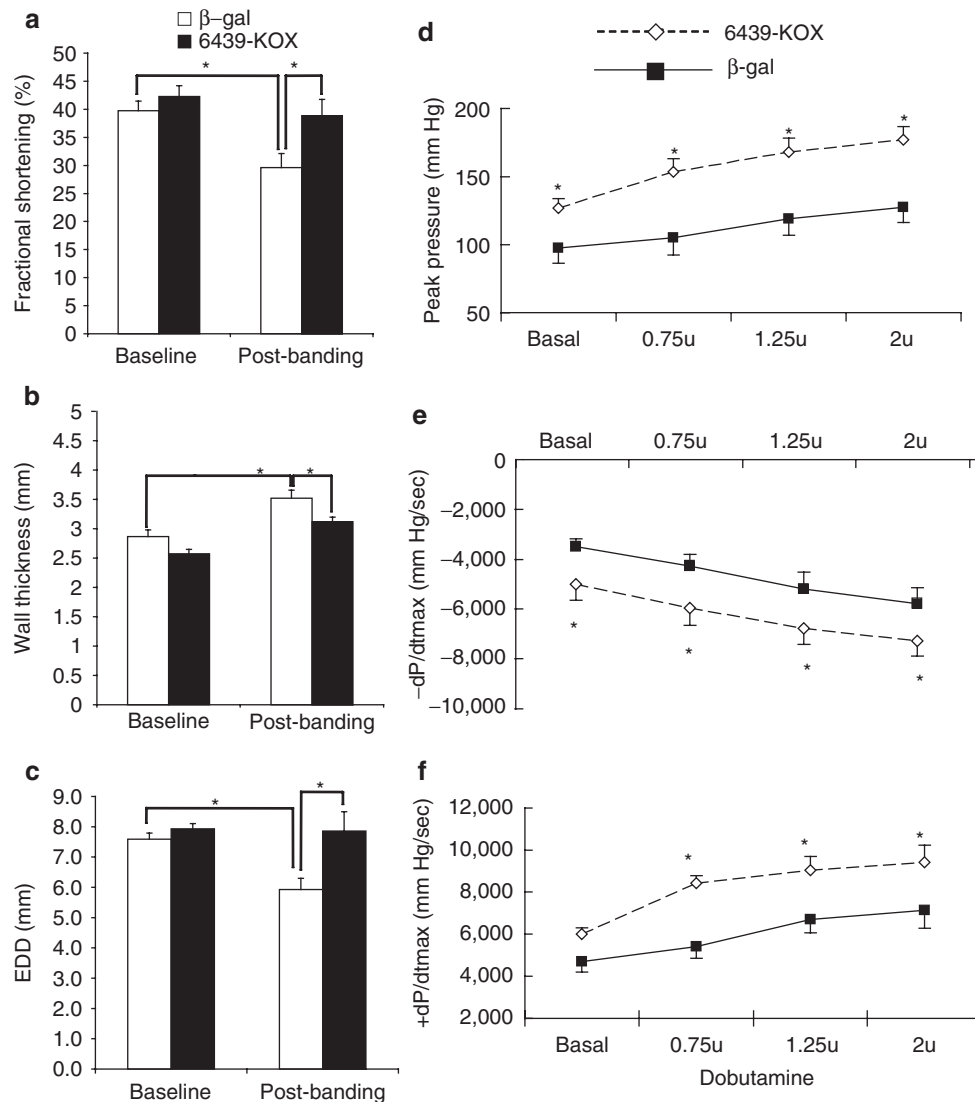


Figure 3 An engineered zinc-finger protein transcription factor (ZFP TF) repressor improves cardiac function *in vivo* in a rat model of heart failure. **(a-c)** AAV-2 vectors encoding either the phospholamban (*PLN*) repressor 6439-KOX or β -gal control were delivered to the hearts of juvenile rats by direct intramyocardial injection. Immediately after gene transfer the rats underwent induction of pressure overload by intrarenal constriction of the abdominal aorta. Four and half-weeks later echocardiography analysis was used to determine **(a)** percent fractional shortening, **(b)** ventricular wall thickness, and **(c)** end-diastolic diameters (EDD); baseline: before aortic banding; post-banding: 4.5 weeks after aortic banding. **(e,f)** Four and half-weeks after gene transfer and induction of pressure overload, myocardial infarction was induced by ligation of the left anterior descending coronary artery. Fourteen-days later terminal hemodynamic analysis was carried out to determine **(d)** peak developed pressures, **(e)** the rate of relaxation ($-dP/dt$), and **(f)** the rate of systolic pressure generation ($+dP/dt$), both at baseline and during infusion of the inotropic drug dobutamine at graduated doses. ($n = 11$ for the 6439-KOX group; $n = 10$ for the β -gal group; $*P$ value <0.05).

studies with concomitant pharmacological stress (dobutamine, a β -adrenergic agonist) revealed significantly greater peak developed ventricular pressures (Figure 3d) and higher rates of intraventricular pressure change during both relaxation and contraction in animals injected with AAV-ZFP6439-KOX ($-dP/dt$ and $+dP/dt$, respectively; Figure 3e, f), although heart rates were not different between the groups. Together these data confirm that ZFP TF repression of the endogenous *PLN* gene results in the expected alterations in cardiac contractility and function.

DISCUSSION

We report the development of a highly specific ZFP TF engineered to bind a *DNaseI*-accessible region of the rat *PLN*

promoter. This ZFP TF potently represses *PLN* transcription in multiple cell types and functionally reduces *PLN* protein levels as gauged by western blot analysis as well as measurements of Ca^{2+} transients and contractility in ZFP-treated rat cardiomyocytes. DNA microarray analysis reveals that the specificity of the *PLN* repressor approaches the level of single-gene regulation within the monitored genome. Moreover, the ZFP repressor is active *in vivo*: in a rat model of heart failure, ZFP delivery improves several measures of cardiac performance that are consistent with functional repression of *PLN*. These data thus provide an important proof-of-concept that ZFP-mediated gene repression may be employed *in vivo* for the potential treatment of heart failure.

The cardiac benefits of increased calcium flux into the sarcoplasmic reticulum are well-established,²⁰ and modulation of PLN and/or SERCA2a activity levels has been highlighted as an attractive strategy for improving calcium handling with minimal collateral effects. This recognition has driven interest in diverse approaches for increasing the SERCA2/PLN ratio, including cardiac delivery of SERCA2a cDNA, a dominant-negative PLN variant as well as RNAi against PLN, which all have been shown to improve contractile properties and prevent the progression of heart failure in animal models.^{14,19,27} Indeed, a SERCA2a gene therapy approach has been shown to be safe and improved cardiac function in early and mid-stage human clinical trials for congestive heart failure.^{28,29} The ZFP repressor that we have developed provides a new approach for increasing SERCA2a activity and improving calcium handling, therefore potentially expanding our options for this serious disease.

A particularly encouraging result in the current work relates to the potency of the effects observed using the *PLN*-specific ZFP repressor despite the relatively modest efficiency of myocardial delivery (Supplementary Figure S3). Even such restricted delivery of the ZFP repressor to the anterior and lateral walls of the left ventricle led to improved measures of cardiac function. While more efficient delivery to a much larger proportion of the myocardium is likely to be required for maximum efficacy, especially in human subjects, delivery methods that improve the transduction efficiency of the myocardium (e.g., catheter-based antegrade or retrograde intracoronary myocardial gene transfer^{30–32}), as well as alternative AAV serotypes that improve transduction efficiency in heart³³ have been described for this purpose.

Beyond repressing *PLN* expression, our study provides direct *in vivo* evidence that “subtractive” therapy, by far the most common mode of action for existing drugs, can be achieved against a recalcitrant drug target (through targeting its genomic DNA) by an engineered ZFP repressor. This result has significant implications for our ability to therapeutically modulate otherwise refractory drug targets in the heart and other organs and tissues. For many such targets (exemplified by *PLN*), subcellular location (e.g., within organellar membranes) or mechanism-of-action (e.g., as a ligand) render the protein product resistant to inhibition via small molecule or antibody-based methods. For other recalcitrant targets, the presence of dozens if not hundreds of other highly similar family members (e.g., kinases, ion channels) can confound attempts to develop inhibitors with sufficient selectivity for therapeutic use. Engineered ZFP repressors circumvent such limitations since the diverse nature of small molecule drug–target interactions can be reduced to a well-understood array of protein–DNA contacts for any drug target. Moreover, due to the higher degree of genetic drift that occurs within regulatory (noncoding) regions of the genome compared to that of coding regions, even genes encoding highly related protein family members are likely to possess unique DNA sequences in their promoters that can be targeted with high specificity by engineered ZFPs.

While engineered ZFPs regulate gene expression by exploiting the natural mechanism of transcription, RNAi-based approaches provide a different way of inhibiting difficult drug targets by triggering the degradation of the mRNA encoding the gene product. For phenotypic penetrance RNAi may need to address the many hundreds (potentially thousands) of copies of the mRNA expressed

from the target gene. In contrast, the ZFP TF approach addresses the source of this message—namely the DNA template, which is present at two copies per cell (for autosomal genes). Moreover, by targeting 18-bp sites and using simple bioinformatics approaches to avoid targeting repetitive sequences, ZFP-driven gene regulation can be highly specific. Because specificity data was not provided for siRNA against *PLN*,²⁷ we cannot directly compare that to the specificity of the ZFP. Nevertheless, this report adds to a growing list of ZFPs developed by our group and others that demonstrate exquisite specificity,^{5,22,34} which compares favorably to that reported for RNAi-based methods.^{35–37} Notably a recent study of *PLN* shRNA in healthy canines revealed cardiac toxicity that the investigators attribute to shRNA-induced perturbation of miRNA expression rather than downregulation of *PLN* activity.³⁸ ZFP-driven *PLN* repression as a direct transcriptional repressor offers an alternative strategy for *PLN* inhibition that does not engage the RNAi processing machinery. This approach thus warrants testing for safety and efficacy in larger animals.

Finally, in striving to extend our therapeutic options to include the genome as a *bona fide* drug target, the versatility of DNA recognition permitted by designed transcription factors is paramount. The C_2H_2 class of ZFPs possess a combination of modularity and adaptability that is unmatched in nature.^{39,40} During the past decade we, and others, have engineered ZFPs for specific targeting of numerous genes (reviewed in refs. 1,41,42). Given this versatility and the therapeutic benefits of targeting genomic DNA, designed ZFPs have the potential of becoming a new class of drugs capable of potent and selective modulation of virtually any therapeutic gene target.

MATERIALS AND METHODS

Mapping of DNaseI-accessible regions. Nuclei isolation from H9C2(2-1) cells, DNaseI treatment, genomic DNA isolation, restriction enzyme digestion and Southern blot analysis were performed as described.³

ZFP design and construction. To target the DNaseI hypersensitive region of the rat *PLN* gene, six-finger ZFP TFs were assembled as described.^{21,43} The resultant ZFP gene was cloned into the pcDNA3.1 vector (Invitrogen, Grand Island, NY) as a fusion with the KRAB A/B transcriptional repression domain of KOX1 as previously described.²² The amino acid residues of the helical regions of ZFP-6439 responsible for specific DNA binding (Fingers 1–6) are TSADLTE, ASANLSR, RSDALST, DRSTRTK, RSDVLSA, and DRSNRIK. The binding site of ZFP-6439 is: GACATGGCCATGGATAGC.

Generation of viral vectors. Recombinant adenoviral vectors encoding 6439-Kox and Kox were generated using the Adeno-X Express System (Clontech, Mountain View, CA). Adenoviral particle numbers were determined by absorbance at 260 nm and infectious titers were determined using the Adeno-X Rapid Titer Kit (Clontech).

Recombinant adeno-associated vectors encoding 6439-kox and β -gal were generated using the triple transfection method as described.⁴⁴

Cell culture and transient transfection. H9C2(2-1) cells were cultured in Dulbecco’s modified Eagle’s medium with 10% fetal bovine serum. Duplicate transfections were performed for each construct using FuGene 6 (Promega, Madison, WI). Cells were harvested 48–72 hours post-transfection for RNA isolation or making whole cell extract. For Affymetrix analysis, $\sim 1 \times 10^6$ cells H9C2(2-1) cells were transfected in duplicate with 7 μ g of ZFP6439-KOX or pcDNA3 empty vector. Cells were harvested 60 hours after transfection. Neonatal and adult rat cardiac myocytes were prepared as previously described.^{18,24}

Real-time reverse transcription-PCR analysis. Real-time reverse transcription-PCR was performed as previously described.⁵ The levels of PLN mRNA and GAPDH mRNA were quantified using standard curves spanning a 125-fold concentration range. Each RNA sample was assayed in duplicate Taqman reactions. The ratio of PLN/GAPDH was used to determine the normalized levels of PLN.

Western blot analysis. Seventy-two hours after transfection of H9C2(2-1) cells or infection of rat cardiomyocytes, whole cell extracts were analyzed by western blot as previously described²² using a monoclonal anti-PLN antibody (Upstate Biotech, Billerica, MA). A polyclonal anti-TFIIB or anti- β -actin antibody (Santa Cruz Biotech, Santa Cruz, CA) was used for internal loading control.

Affymetrix analysis. Total RNA was isolated from transfected H9C2(2-1) cells using TRIzol reagent (Invitrogen) according to manufacturer's recommendations. RNA samples for hybridization were prepared according to standard Affymetrix protocol using 10 μ g of total RNA. Changes in gene expression were analyzed using rat RAE-230A array, which contains 15,923 probes representing roughly 14,000 genes. Data analysis was carried out using Affymetrix Microarray Suite 5.0 and Data Mining Tool 3.0 software. Criteria for differentially expressed genes were: 100% confidence call, and *P* value <0.05.

Single-cell Ca^{2+} transient analysis. Neonatal cardiomyocytes from Sprague Dawley rats were infected with Ad-6439-KOX or Ad-KOX at MOI 200 in a Petri dish invested with platinum electrodes and placed on the heated stage of a Zeiss Axiovert 135 inverted microscope fitted with a Delta Scan Photometry system (Photon Technology International, Lawrenceville, NJ) for measurement of calcium transients. The cells were paced at a rate of 1 Hz. Fluo-3 (Molecular Probes, San Diego, CA) was loaded into myocytes according to the manufacturer's recommendations and was used as an indicator of cytosolic calcium. Calcium transients were captured using Felix software (Photon Technology International) and background subtracted. The time for intracellular calcium to decrease to 50% of maximum amplitude ($T_{1/2}$) was determined as described.^{18,24}

Single-cell contractility analysis. Sprague Dawley rats were treated humanely in accordance with federal and Yale School of Medicine policies regarding the use of animals in research. Ad-6439-KOX or Ad-KOX (2.5×10^9 pfu) were coinjected along with an adenovirus encoding a fluorescent marker, Ad-FS-Red (2.5×10^9 pfu), directly into the myocardium of rats via a lateral thoracotomy as previously described.⁴⁵ Seventy-two hours later rod-shaped cardiac myocytes were isolated from these hearts by collagenase digestion as described.²⁴ Isolated cardiac myocytes were paced at 1 Hz, and a video edge detection system (Crescent Electronics, Windsor, Ontario, Canada) measured the magnitude of cell shortening. The percentage of cell shortening was expressed as $([\text{basal length} - \text{contracted length}] / \text{basal length}) \times 100$. Rates of contraction and relaxation were calculated as basal length—shortest length/time from basal to shortest length (+dP/dt); and shortest length—basal length/time from shortest to basal length during relaxation –dP/dt).

In vivo transduction with AAV vectors. Myocardial gene delivery was accomplished by direct intramyocardial injection with a modified 30 gauge bore needle. Briefly, in anesthetized and ventilated rats the heart was exposed by lateral thoracotomy. The modified needle was fashioned with a near 90 angle at the distal tip to facilitate entry into the myocardium through the thoracotomy. AAV- β -gal or AAV-6439-KOX (5×10^{11} AAV vector genomes) was injected at six separate sites in a total of 200 μ l of phosphate-buffered saline (volume equally divided amongst the sites). After injection the chest was closed in layers, and air evacuated from the pleural space via a cannula left in place during chest closure.

Induction of pressure overload, myocardial infarction, echocardiography, and hemodynamic analysis. All *in vivo* experiments were performed according to protocols approved by the IACUC at Yale Medical School.

Abdominal aortic banding was accomplished by a transabdominal surgical approach. The infrarenal abdominal aorta was visualized and a silk ligature placed around it and an 18-gauge needle angled at the tip. After ligation the needle was removed and the abdominal closed in layers. The degree of stenosis and documentation of flow to the aorta beyond the constriction was determined by ultrasound and Doppler imaging. Transthoracic echocardiography was performed 4.5 weeks later under inhaled anesthesia (isoflurane) using a 7.5 MHz transducer.^{24,46} Following echocardiography myocardial infarction was induced by lateral thoracotomy followed by ligation of the left anterior descending coronary artery just after the first branch. Ligation and cessation of myocardial flow in that territory was confirmed by visualization of myocardial blanching. The chest was then closed in layers and the animals allowed to recover. Fourteen-days after infarction cardiac function was assessed by terminal hemodynamic studies in ventilated animals under isoflurane anesthesia, using a microtransducer-tipped catheter inserted into the left ventricle via the carotid artery. Graduated doses of dobutamine were infused at a constant rate via a syringe pump and a cannula in the internal jugular vein.⁴⁶

SUPPLEMENTARY MATERIAL

Figure S1. Catecholamine-O-methyltransferase expression is not regulated by the PLN repressor.

Figure S2. Efficiency of coinfection following intramuscular injection of two separate adenovirus vectors.

Figure S3. AAV-mediated delivery following direct intramyocardial injection.

Supplementary Materials and Methods.

ACKNOWLEDGMENTS

We thank Ken Kim, Kathie Howes, and Simon Chandler for ZFP assembly; Albert Sinusas for assistance with the rat model, Fyodor Urnov, Susan Abrahamson, and Lei Zhang for helpful discussions and comments, and Edward Lanphier for encouragement and support. This study is supported in part by NIH NHLBI grants HL64001 and HL63770 to F.J.G. H.S.Z., D.G., M.K., S.H., Y.L., L.H., S.K.S., C.C.C., E.J.R., and P.D.G. are employees of Sangamo BioSciences Inc.

REFERENCES

- Klug, A (2005). Towards therapeutic applications of engineered zinc finger proteins. *FEBS Lett* **579**: 892–894.
- Lu, Y, Tian, C, Daniailou, G, Gilbert, R, Petrof, BJ, Karpati, G *et al.* (2008). Targeting artificial transcription factors to the utrophin A promoter: effects on dystrophic pathology and muscle function. *J Biol Chem* **283**: 34720–34727.
- Rebar, EJ, Huang, Y, Hickey, R, Nath, AK, Meoli, D, Nath, S *et al.* (2002). Induction of angiogenesis in a mouse model using engineered transcription factors. *Nat Med* **8**: 1427–1432.
- Laganier, J, Kells, AP, Lai, JT, Guschin, D, Paschon, DE, Meng, X *et al.* (2010). An engineered zinc finger protein activator of the endogenous glial cell line-derived neurotrophic factor gene provides functional neuroprotection in a rat model of Parkinson's disease. *J Neurosci* **30**: 16469–16474.
- Yokoi, K, Zhang, HS, Kachi, S, Balaggan, KS, Yu, Q, Guschin, D *et al.* (2007). Gene transfer of an engineered zinc finger protein enhances the anti-angiogenic defense system. *Mol Ther* **15**: 1917–1923.
- Kang, YA, Shin, HC, Yoo, JY, Kim, JH, Kim, JS and Yun, CO (2008). Novel cancer antiangiotherapy using the VEGF promoter-targeted artificial zinc-finger protein and oncolytic adenovirus. *Mol Ther* **16**: 1033–1040.
- Mussolino, C, Sanges, D, Marrocco, E, Bonetti, C, Di Vicino, U, Marigo, V *et al.* (2011). Zinc-finger-based transcriptional repression of rhodopsin in a model of dominant retinitis pigmentosa. *EMBO Mol Med* **3**: 118–128.
- MacLennan, DH and Kranias, EG (2003). Phospholamban: a crucial regulator of cardiac contractility. *Nat Rev Mol Cell Biol* **4**: 566–577.
- Frank, KF, Böck, B, Erdmann, E and Schwinger, RH (2003). Sarcoplasmic reticulum Ca^{2+} -ATPase modulates cardiac contraction and relaxation. *Cardiovasc Res* **57**: 20–27.
- Haghighi, K, Chen, G, Sato, Y, Fan, GC, He, S, Kolokathis, F *et al.* (2008). A human phospholamban promoter polymorphism in dilated cardiomyopathy alters transcriptional regulation by glucocorticoids. *Hum Mutat* **29**: 640–647.
- Haghighi, K, Kolokathis, F, Gramolini, AO, Waggoner, JR, Pater, L, Lynch, RA *et al.* (2006). A mutation in the human phospholamban gene, deleting arginine 14, results in lethal, hereditary cardiomyopathy. *Proc Natl Acad Sci USA* **103**: 1388–1393.
- Minamisawa, S, Sato, Y, Tatsuguchi, Y, Fujino, T, Imamura, S, Uetsuka, Y *et al.* (2003). Mutation of the phospholamban promoter associated with hypertrophic cardiomyopathy. *Biochem Biophys Res Commun* **304**: 1–4.
- Nef, HM, Möllmann, H, Skwara, W, Böck, B, Schwinger, RH, Hamm, Ch *et al.* (2006). Reduced sarcoplasmic reticulum Ca^{2+} -ATPase activity and dephosphorylated

- phospholamban contribute to contractile dysfunction in human hibernating myocardium. *Mol Cell Biochem* **282**: 53–63.
14. del Monte, F, Williams, E, Lebeche, D, Schmidt, U, Rosenzweig, A, Gwathmey, JK *et al.* (2001). Improvement in survival and cardiac metabolism after gene transfer of sarcoplasmic reticulum Ca(2+)-ATPase in a rat model of heart failure. *Circulation* **104**: 1424–1429.
 15. Hajjar, RJ, Schmidt, U, Matsui, T, Guerrero, JL, Lee, KH, Gwathmey, JK *et al.* (1998). Modulation of ventricular function through gene transfer *in vivo*. *Proc Natl Acad Sci USA* **95**: 5251–5256.
 16. Luo, W, Grupp, IL, Harrer, J, Ponniah, S, Grupp, G, Duffy, JJ *et al.* (1994). Targeted ablation of the phospholamban gene is associated with markedly enhanced myocardial contractility and loss of beta-agonist stimulation. *Circ Res* **75**: 401–409.
 17. He, H, Meyer, M, Martin, JL, McDonough, PM, Ho, P, Lou, X *et al.* (1999). Effects of mutant and antisense RNA of phospholamban on SR Ca(2+)-ATPase activity and cardiac myocyte contractility. *Circulation* **100**: 974–980.
 18. Giordano, FJ, He, H, McDonough, P, Meyer, M, Sayen, MR and Dillmann, WH (1997). Adenovirus-mediated gene transfer reconstitutes depressed sarcoplasmic reticulum Ca2+-ATPase levels and shortens prolonged cardiac myocyte Ca2+ transients. *Circulation* **96**: 400–403.
 19. Hoshijima, M, Ikeda, Y, Iwanaga, Y, Minamisawa, S, Date, MO, Gu, Y *et al.* (2002). Chronic suppression of heart-failure progression by a pseudophosphorylated mutant of phospholamban via *in vivo* cardiac rAAV gene delivery. *Nat Med* **8**: 864–871.
 20. Chien, KR, Ross, J Jr and Hoshijima, M (2003). Calcium and heart failure: the cycle game. *Nat Med* **9**: 508–509.
 21. Moore, M, Choo, Y and Klug, A (2001). Design of polyzinc finger peptides with structured linkers. *Proc Natl Acad Sci USA* **98**: 1432–1436.
 22. Tan, S, Guschin, D, Davalos, A, Lee, YL, Snowden, AW, Jouvenot, Y *et al.* (2003). Zinc-finger protein-targeted gene regulation: genomewide single-gene specificity. *Proc Natl Acad Sci USA* **100**: 11997–12002.
 23. Frank, S, Gauster, M, Strauss, J, Hrsenjak, A and Kostner, GM (2001). Adenovirus-mediated apo(a)-antisense-RNA expression efficiently inhibits apo(a) synthesis *in vitro* and *in vivo*. *Gene Ther* **8**: 425–430.
 24. Huang, Y, Hickey, RP, Yeh, JL, Liu, D, Dadak, A, Young, LH *et al.* (2004). Cardiac myocyte-specific HIF-1alpha deletion alters vascularization, energy availability, calcium flux, and contractility in the normoxic heart. *FASEB J* **18**: 1138–1140.
 25. Reddy, DS, Singh, M, Ghosh, S and Ganguly, NK (1996). Role of cardiac renin-angiotensin system in the development of pressure-overload left ventricular hypertrophy in rats with abdominal aortic constriction. *Mol Cell Biochem* **155**: 1–11.
 26. Nakayama, H, Otsu, K, Yamaguchi, O, Nishida, K, Date, MO, Hongo, K *et al.* (2003). Cardiac-specific overexpression of a high Ca2+ affinity mutant of SERCA2a attenuates *in vivo* pressure overload cardiac hypertrophy. *FASEB J* **17**: 61–63.
 27. Suckau, L, Fechner, H, Chemaly, E, Krohn, S, Hadri, L, Kockskämper, J *et al.* (2009). Long-term cardiac-targeted RNA interference for the treatment of heart failure restores cardiac function and reduces pathological hypertrophy. *Circulation* **119**: 1241–1252.
 28. Jaski, BE, Jessup, ML, Mancini, DM, Cappola, TP, Pauly, DF, Greenberg, B *et al.*; Calcium Up-Regulation by Percutaneous Administration of Gene Therapy In Cardiac Disease (CUPID) Trial Investigators. (2009). Calcium upregulation by percutaneous administration of gene therapy in cardiac disease (CUPID Trial), a first-in-human phase 1/2 clinical trial. *J Card Fail* **15**: 171–181.
 29. Jessup, M, Greenberg, B, Mancini, D, Cappola, T, Pauly, DF, Jaski, B *et al.*; Calcium Upregulation by Percutaneous Administration of Gene Therapy in Cardiac Disease (CUPID) Investigators. (2011). Calcium upregulation by Percutaneous Administration of Gene Therapy in Cardiac Disease (CUPID): a phase 2 trial of intracoronary gene therapy of sarcoplasmic reticulum Ca2+-ATPase in patients with advanced heart failure. *Circulation* **124**: 304–313.
 30. Hou, D, Maclaughlin, F, Thiesse, M, Panchal, VR, Bekkers, BC, Wilson, EA *et al.* (2003). Widespread regional myocardial transfection by plasmid encoding Del-1 following retrograde coronary venous delivery. *Catheter Cardiovasc Interv* **58**: 207–211.
 31. Kaye, DM, Prevolos, A, Marshall, T, Byrne, M, Hoshijima, M, Hajjar, R *et al.* (2007). Percutaneous cardiac recirculation-mediated gene transfer of an inhibitory phospholamban peptide reverses advanced heart failure in large animals. *J Am Coll Cardiol* **50**: 253–260.
 32. Giordano, FJ (2003). Retrograde coronary perfusion: a superior route to deliver therapeutics to the heart?*. *J Am Coll Cardiol* **42**: 1129–1131.
 33. Wang, Z, Zhu, T, Qiao, C, Zhou, L, Wang, B, Zhang, J *et al.* (2005). Adeno-associated virus serotype 8 efficiently delivers genes to muscle and heart. *Nat Biotechnol* **23**: 321–328.
 34. Guan, X, Stege, J, Kim, M, Dahmani, Z, Fan, N, Heifetz, P *et al.* (2002). Heritable endogenous gene regulation in plants with designed polydactyl zinc finger transcription factors. *Proc Natl Acad Sci USA* **99**: 13296–13301.
 35. Doench, JG, Petersen, CP and Sharp, PA (2003). siRNAs can function as miRNAs. *Genes Dev* **17**: 438–442.
 36. Jackson, AL, Bartz, SR, Schelter, J, Kobayashi, SV, Burchard, J, Mao, M *et al.* (2003). Expression profiling reveals off-target gene regulation by RNAi. *Nat Biotechnol* **21**: 635–637.
 37. Lin, X, Ruan, X, Anderson, MG, McDowell, JA, Kroeger, PE, Fesik, SW *et al.* (2005). siRNA-mediated off-target gene silencing triggered by a 7 nt complementation. *Nucleic Acids Res* **33**: 4527–4535.
 38. Bish, LT, Sleeper, MM, Reynolds, C, Gazzara, J, Withnall, E, Singletary, GE *et al.* (2011). Cardiac gene transfer of short hairpin RNA directed against phospholamban effectively knocks down gene expression but causes cellular toxicity in canines. *Hum Gene Ther* **22**: 969–977.
 39. Pabo, CO, Peisach, E and Grant, RA (2001). Design and selection of novel Cys2His2 zinc finger proteins. *Annu Rev Biochem* **70**: 313–340.
 40. Segal, DJ, Beerli, RR, Blancafort, P, Dreier, B, Effertz, K, Huber, A *et al.* (2003). Evaluation of a modular strategy for the construction of novel polydactyl zinc finger DNA-binding proteins. *Biochemistry* **42**: 2137–2148.
 41. Jamieson, AC, Miller, JC and Pabo, CO (2003). Drug discovery with engineered zinc-finger proteins. *Nat Rev Drug Discov* **2**: 361–368.
 42. Visser, AE, Verschure, PJ, Gommans, WM, Haisma, HJ and Rots, MG (2006). Step into the groove: engineered transcription factors as modulators of gene expression. *Adv Genet* **56**: 131–161.
 43. Moore, M, Klug, A and Choo, Y (2001). Improved DNA binding specificity from polyzinc finger peptides by using strings of two-finger units. *Proc Natl Acad Sci USA* **98**: 1437–1441.
 44. Matsushita, T, Elliger, S, Elliger, C, Podsakoff, G, Villarreal, L, Kurtzman, GJ *et al.* (1998). Adeno-associated virus vectors can be efficiently produced without helper virus. *Gene Ther* **5**: 938–945.
 45. Abbott, JD, Huang, Y, Liu, D, Hickey, R, Krause, DS and Giordano, FJ (2004). Stromal cell-derived factor-1alpha plays a critical role in stem cell recruitment to the heart after myocardial infarction but is not sufficient to induce homing in the absence of injury. *Circulation* **110**: 3300–3305.
 46. Lei, L, Mason, S, Liu, D, Huang, Y, Marks, C, Hickey, R *et al.* (2008). Hypoxia-inducible factor-dependent degeneration, failure, and malignant transformation of the heart in the absence of the von Hippel-Lindau protein. *Mol Cell Biol* **28**: 3790–3803.



This work is licensed under the Creative Commons Attribution-NonCommercial-NoDerivative Works 3.0 Unported License. To view a copy of this license, visit <http://creativecommons.org/licenses/by-nc-nd/3.0/>